Journal of the European Ceramic Society **19** (1999) 2005–2013

PII: S0955-2219(99)00008-4
0955-2219/99/$ - see front matter

Electrical Properties of Sputtered PZT Films on Stabilized Platinum Electrode

G. Vélu and D. Rèmiens*

Laboratoire des Matériaux Avancés Céramiques (LAMAC), Université de Valenciennes et du Hainaut-Cambrésis, Z.I. Champ de l'Abbesse, 59600 Maubeuge, France

(Received 20 May 1998; accepted 30 December 1998)

Abstract

PZT (54/46) thin films were deposited by r.f. magnetron sputtering followed by a post-annealing treatment on silicon substrates. The crucial role of a Ti adhesion layer on the Ti/Pt bottom electrode is presented. The deposition conditions and the thickness of Ti have dominant effects on the interactions between Ti and Pt during the annealing treatment. The Pt layer, whatever its thickness, did not act as a barrier against Ti-out diffusion. The stability of the bottom electrode was achieved by using a TiO_x layer instead of a pure metallic Ti adhesion layer. The electrical properties of PZT films in terms of dielectric and ferroelectric performance were evaluated, particularly as a function of the PZT film thickness.

Keywords: sputtering, films, electrical properties, PZT, TiO_2.

Resumé

Des films minces de PZT (54/46) ont été déposés sur des substrats de silicium par pulvérisation cathodique r.f. magnétron. Le rôle de la couche d'accrochage de titane au niveau de l'électrode inférieure Ti/Pt est présenté. Les conditions de dépôt et l'épaisseur de la couche de Ti ont des effets importants sur les interactions entre le titane et le platine durant le traitement thermique du PZT. Le film de platine, quelle que soit son épaisseur ne joue pas le rôle de couche barrière à la diffusion du titane. La stabilité de l'électrode inférieure est obtenue en remplacant le Ti par TiO_x. Les propriétés électriques des films de PZT en termes de performances diélectriques et ferroélectriques sont évaluées. En particulier, nous avons étudié leur dépendence avec l'épaisseur des films de PZT.

*To whom correspondence should be addressed.

1 Introduction

Ferroelectric lead zirconate titanate Pb(Zr, Ti)O_3 (PZT) film is one of the promising materials applicable to a variety of devices including semiconductor non-volatile memories,[1] piezoelectric ultrasonic micromotors,[2] pyroelectric detectors[3] and capacitors in Dynamic Random Access Memories.[4] For these applications, it is imperative, therefore, that the characteristics of the metal–ferroelectric–metal (MFM) structures be investigated systematically to determine the influence of the bottom electrode on the film properties and their dependence on the PZT film thickness.

The electrode material plays an important role in determining film performance. In thin film form, the influence of the electrode–ferroelectric interface is more pronounced when compared with bulk ceramic.[5] A Ti/Pt bilayer is the most widely chosen electrode for Si-based devices because Pt is relatively inert to oxygen. The Ti layer is necessary to promote the adhesion of Pt to SiO_2.

The major problem associated with using platinum bottom electrodes is the interaction with the titanium adhesion layer during the post-annealing treatment of the PZT films.[6,7]

In this study, the Ti and Pt atoms movements were examined before and after different annealing treatments for various deposition conditions of the Ti film. Auger electron spectroscopy (AES) has been applied to clarify the diffusion behavior of each element: Ti, Pt, Si, O. These experimental results are used to define a stabilized bottom electrode where Ti is replaced by TiO_x.

Thickness dependencies of relative permittivity and ferroelectric properties (coercive field, remanent polarization) of sputtered PZT films deposited on stable electrodes were explored through appropriate electrical measurements. The reduction in film thickness leads to a decrease of the permittivity and an increase of the coercive field. We have

also observed a disappearance of the internal electric field when the PZT film thickness increased.

2 Experimental procedure

PZT thin films, with a (Zr, Ti) ratio equal to (54/46) were prepared on stabilized platinized silicon (Si) substrates by r.f. magnetron sputtering; the system deposition has been described previously.[8] Titanium and platinum films were deposited on (100)-oriented Si substrates passivated with a thermally grown silicon dioxide layer of 3000 Å. The bottom electrodes were grown by r.f. magnetron sputtering without substrate heating. They were fabricated by a sequential deposition process in a single pump-down cycle without breaking the vacuum. The growth conditions were fixed in order to have a slow growth rate to produce dense Pt films: an r.f. power of 50 and 70 W for the Ti and Pt films, respectively (the target diameter is 150 mm) and a working pressure (Ar gas) of 5 mT for the two materials. The thickness of the Ti/Pt bilayers, varied between 60 and 240 Å for Ti and 1000 and 2500 Å for Pt. Figure 1 shows a cross-section of the studied structure showing the sequence of layers. The as-deposited Pt layer exhibited a strong (111)-preferred orientation before annealing; this orientation is maintained (reinforced) after processing (see Fig. 8). The evolution of these Ti/Pt electrodes (element diffusion) before PZT deposition was investigated using Auger electron spectroscopy (AES) for different post-annealing treatments and in particular for the annealing treatment used to

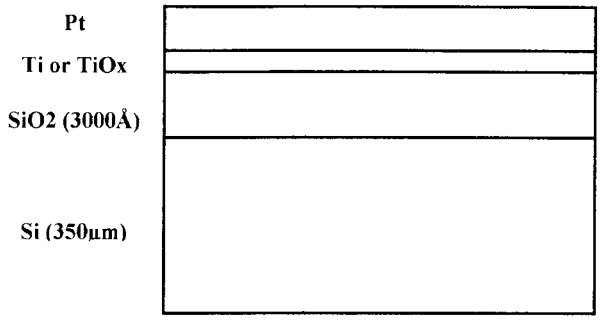

Fig. 1. Cross-section showing the sequence of layers of the substrate used in this study.

Table 1. Sputtering and post-annealing conditions for fabrication of PZT (54/46) films

R. F. power density	2·36 W cm^{-2}
Target diameter	75 mm
Target composition	PZT (54/46) without lead excess
Inter-electrodes distance	60 mm
Gas pressure	30 mT
Sputtering gas	Ar
Substrates temperature	Ambiant
Annealing temperature	650°C
Annealing time	30 min
Heating rate	3°C min^{-1}
Cooling rate	1°C min^{-1}
Gas ambiant	Air

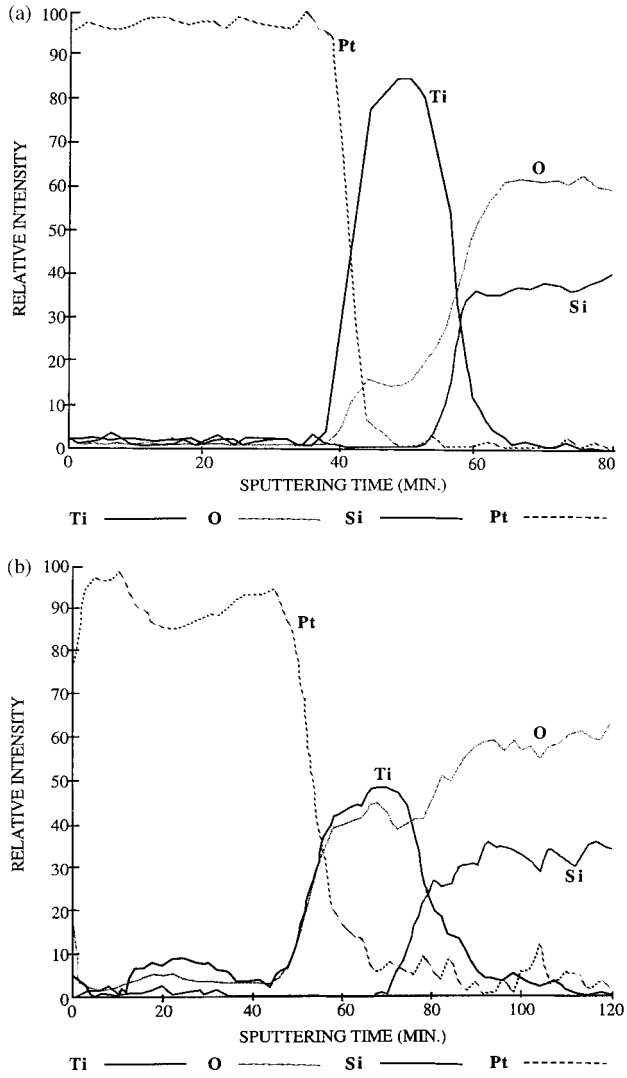

Fig. 2. AES depth profiles of Ti (60 Å)/Pt (1000 Å) electrode: (a) as-deposited, (b) after annealing (650°C, 30 min).

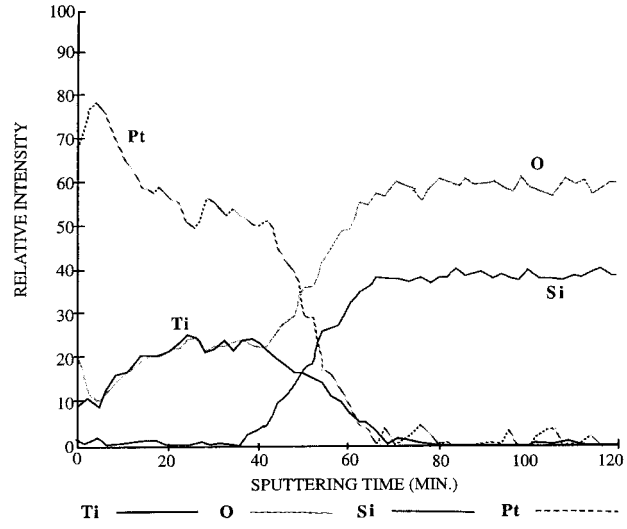

Fig. 3. AES depth profile of Ti (240 Å)/Pt (1000 Å) after annealing (650°C, 30 min).

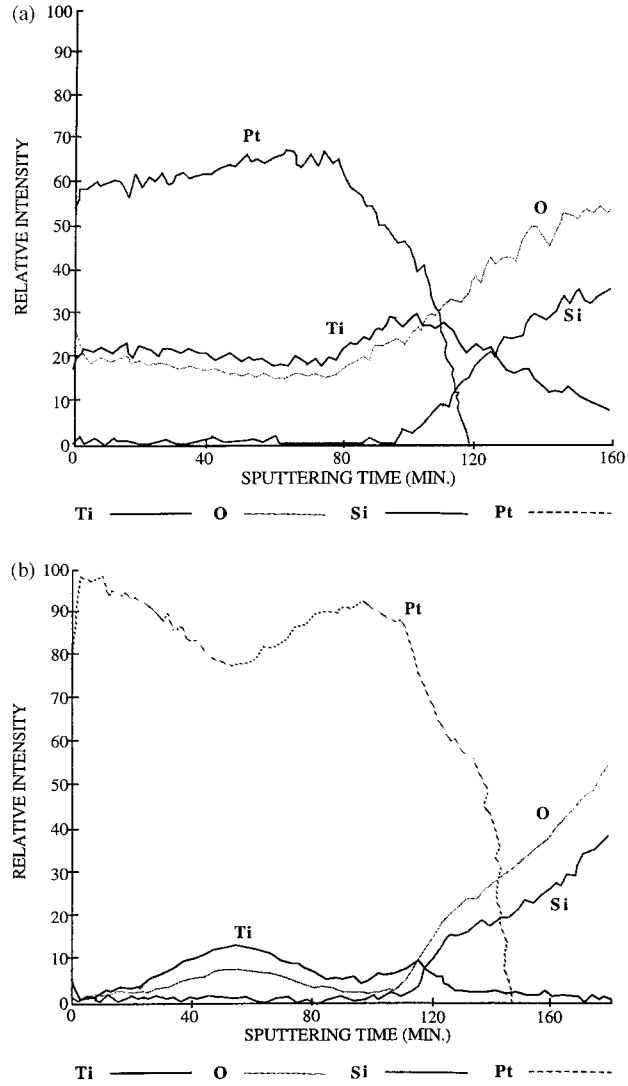

Fig. 4. AES depth profiles of: (a) Ti (240 Å)/Pt (200 Å), (b) Ti (240 Å)/Pt (2500 Å) electrodes after annealing (650°C, 30 min).

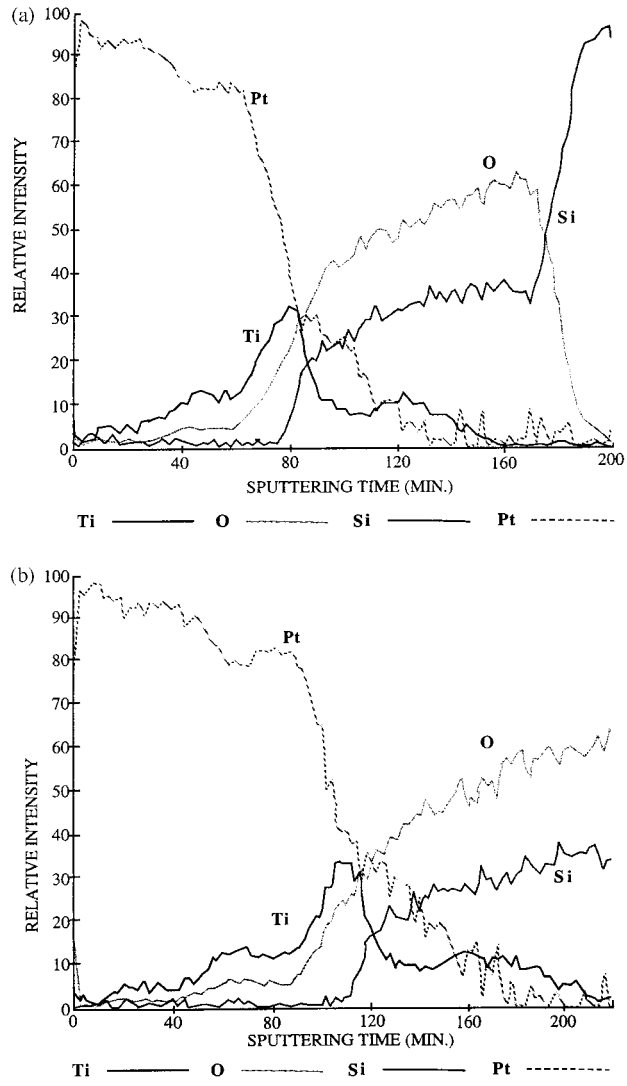

Fig. 5. AES depth profiles of Ti/Pt electrode after annealing at: (a) 550°C, (b) 600°C.

crystallize the PZT films. In order to stabilize the electrode, i.e. to suppress the interactions of Ti with the Pt layer, we have modified the Ti layer growth conditions with the introduction of O_2 in the process to form titanium oxide. The PZT films were deposited at room temperature; the selected sputtering conditions are summarized in Table 1. No lead excess was used in the target. With these parameters, the growth rate is in the order of 50 Å min^{-1} and the films contains a little excess of lead (Pb/Zr + Ti = 1·1). We have made this choice since in general it has been observed that the presence of lead excess in the film favors the perovskite phase formation.[9,10] The lead excess is evaporated during the annealing treatment. The post-annealing parameters are listed in Table 1; the ramp down is fixed to 1°C min^{-1}, for higher values microcracks appear in the films.

The structural phase of the PZT films deposited on different bottom electrodes were compared. The electrical properties of PZT films deposited on stabilized electrodes ($Si/SiO_2/TiO_x/Pt$) were evaluated

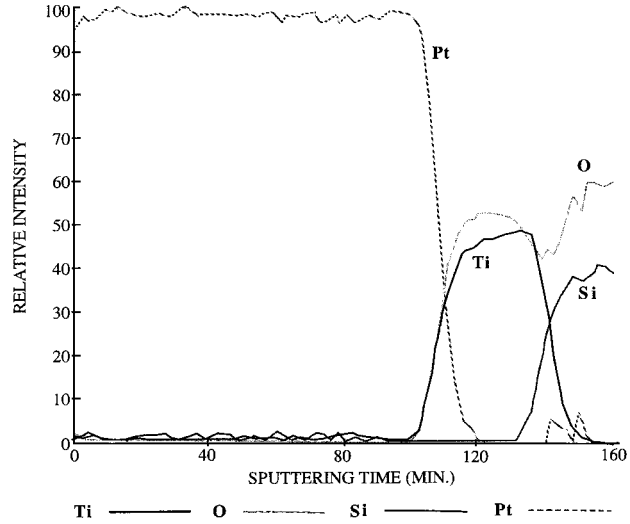

Fig. 6. AES depth profile of TiO_x (100 Å)/Pt (1200 Å) after annealing (650°, 30 min)

and we have studied the evolution of the dielectric constant, the ferroelectric properties (coercive field, remanent polarization...) and the leakage currents with the PZT film thickness.

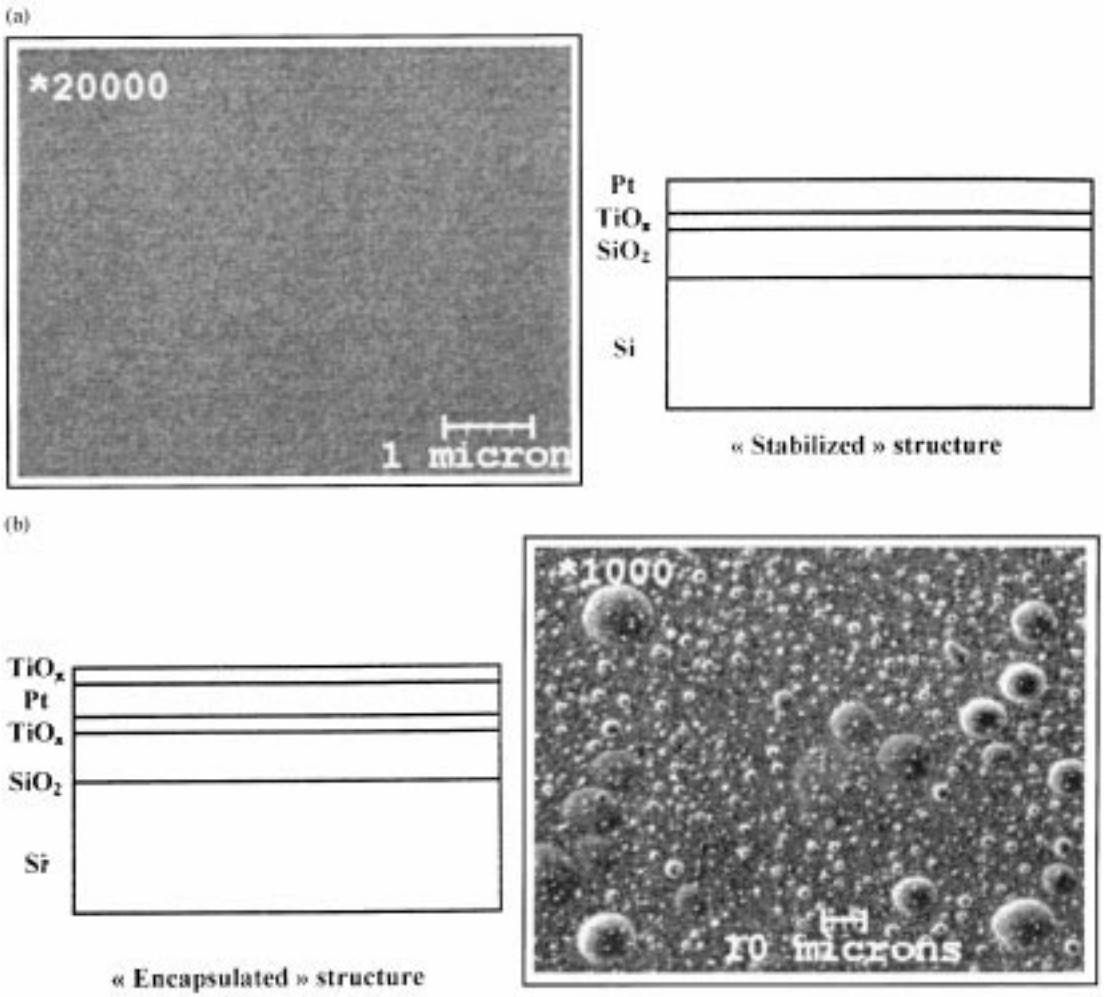

Fig. 7. SEM of the surface morphology of: (a) stabilized, (b) encapsulated electrodes.

3 Results and Discussion

3.1 Post-annealing effects on Ti/Pt bottom electrode stability

To investigate the substrate evolution during the PZT post-annealing treatment, $Si/SiO_2/Ti/Pt$ substrates were annealed at 650°C (in air) during 30 min (which are the conventional PZT annealing treatment parameters) and analysed by AES.

In Fig. 2 the AES depth profiles of an as-deposited [Fig. 2(a)] and annealed [Fig. 2(b)] Ti/Pt electrode are shown; the Ti and Pt layers thicknesses are 60 and 1000 Å, respectively. The post-annealing treatment causes oxidation of the intermediate Ti layer and its migration into Pt. Some Ti atoms reached the opposite surface of the Pt layer and finally accumulated there. This effect is more pronounced by using thicker Ti films as shown in Fig. 3; the Ti layer thickness is 240 Å in this example. The Pt layer was encapsulated by a thin layer of TiO_x; identical results were observed by Sreenivas *et al.*[11] We have increased the Pt layer thickness with the hypothesis that Pt acts as a barrier layer against Ti diffusion and thus prevents the formation of a TiO_x layer at the Pt surface. Figure 4(a) and (b), relative to Pt layer thicknesses of 2000 and 2500 Å, respectively (the Ti layer thickness is maintained constant around 240 Å), shows that, whatever the Pt thickness, the Ti atoms migration occurs and we can conclude that the Pt layer does not play the role of effective diffusion barrier for Ti and oxygen. It is interesting to note that even for lower annealing temperatures [550 and 600°C in Fig. 5(a) and (b), respectively] a redistribution of Ti through Pt was also observed.

These experimental results shows that during the post-annealing treatment, the $Si/SiO_2/Ti/Pt$ substrate was altered into the $Si/SiO_2/TiO_x/Pt$ or $Si/SiO_2/TiO_x/Pt/TiO_x$ structure depending on the Ti film thickness. Decreasing the annealing temperature was ineffective to prevent the migration of Ti through Pt.

Since this modification is essentially attributed to the Ti-out diffusion into the Pt layer, some authors

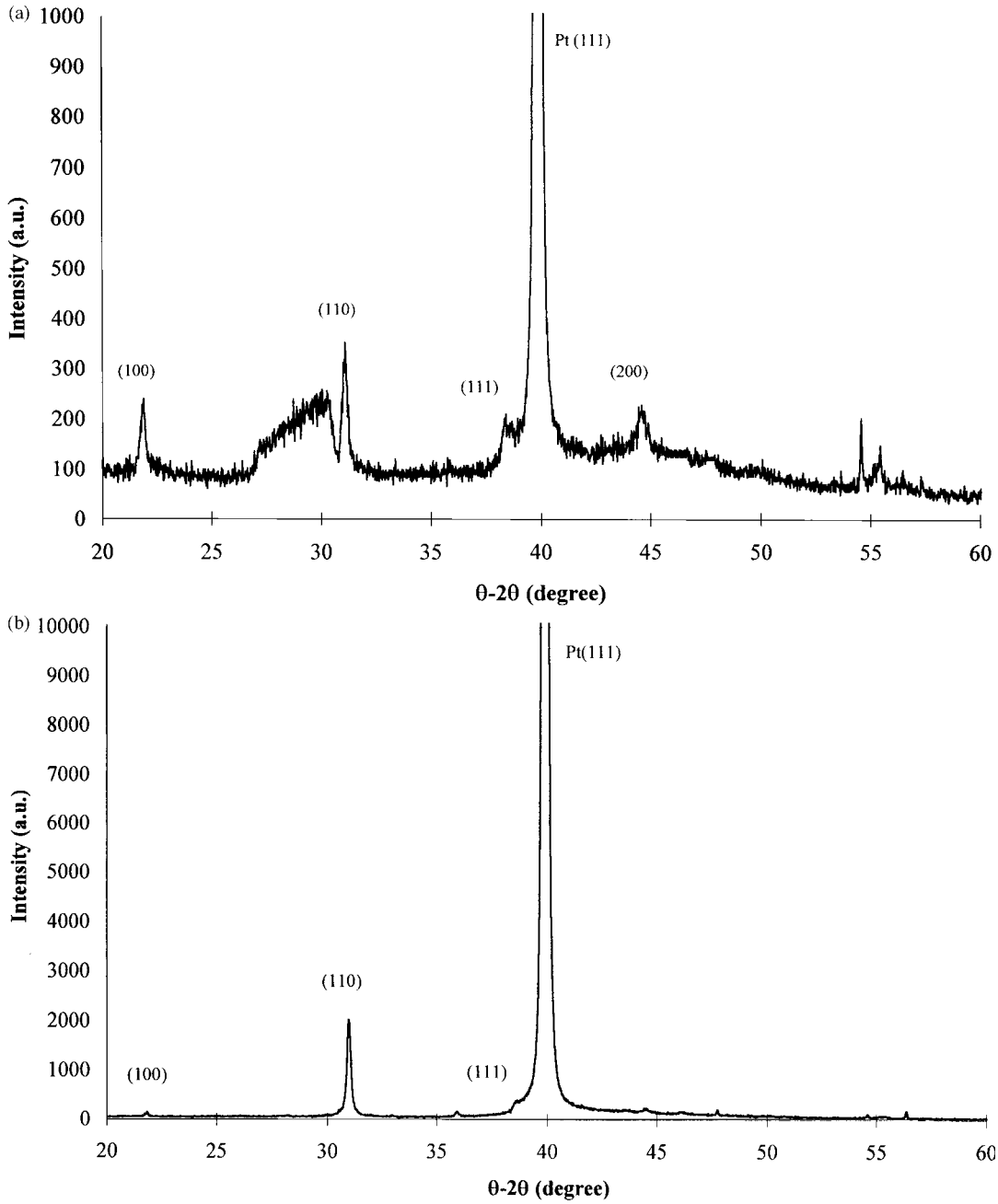

Fig. 8. XRD patterns of a PZT film deposited on: (a) encapsulated, (b) stabilized electrodes.

have proposed to replace the Ti adhesion layer by TiO_2 (or TiO_x). With the modified $Si/SiO_2/TiO_x/Pt$ structure no significant interdiffusion was observed during the annealing treatment.[12,13] We have tested this structure and the results are illustrated by the AES spectrum presented in Fig. 6. We have realized the electrode with two deposition steps. Firstly, we have deposited a Ti layer (100 Å) followed by an annealing treatment (680°C in air) in order to form TiO_x and in a second step a Pt layer (1200 Å) was deposited. Figure 6 shows a stable TiO_x-Pt interface after the annealing treatment of the complete structure, no interdiffusion was observed even for thicker TiO_x film thickness.

Stability of the bottom electrode was achieved by stabilizing the interface chemistry with the formation of a TiO_x layer at the interface instead of pure metallic Ti thin films.

The procedure used to stabilize the bottom electrode is too long (two deposition and annealing steps) and so we have deposited directly TiO_x on SiO_2 by reactive sputtering of a Ti metal target in oxygen. The TiO_x, film thickness is fixed to 300 Å. The surface morphology of a stabilized electrode is presented Fig. 7(a). The surface is smooth without defect. The situation is radically different for an encapsulated electrode [Fig. 7(b)], where the surface is very rough due to the existence of a non continuous TiO_x layer which causes hillock and microcracks formation.[14,15] Platinum hillocks caused some shorting during electrical measurements.[16,17]

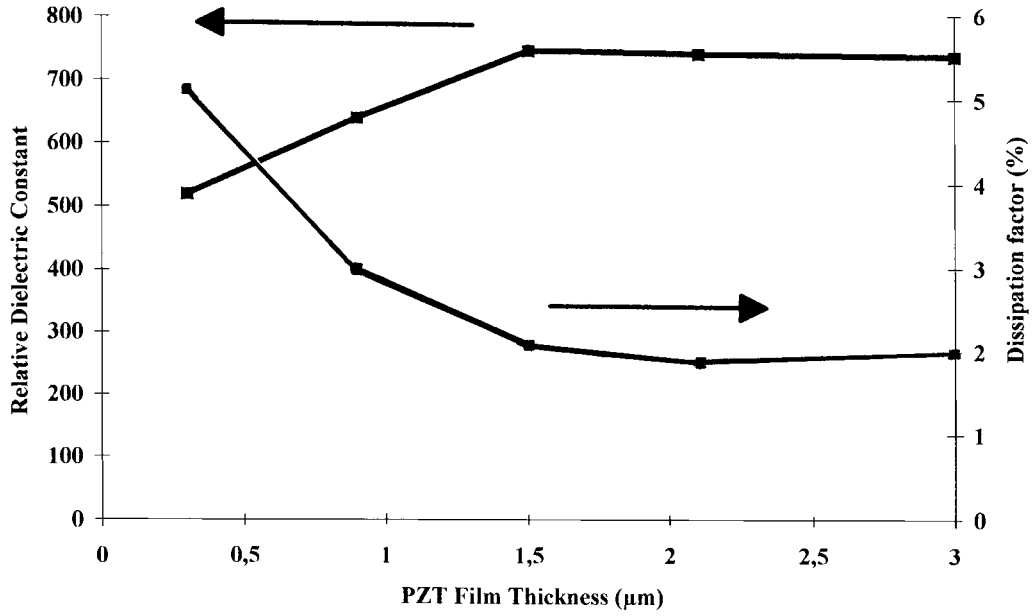

Fig. 9. Relative dielectric constant and dissipation factor as a function of PZT film thickness at 1 kHz.

3.2 Crystallization of PZT films

Amorphous PZT films deposited on encapsulated electrodes, i.e. $Si/SiO_2/TiO_x/Pt/TiO_x$ substrates, and on stabilized electrodes ($Si/SiO_2/TiO_x/Pt$) were post-annealed at 650°C (during 30 min). A representative XRD of a 2500 Å film is shown in Fig. 8. The presence of TiO_x at the interface between Pt and PZT films inhibits the perovskite phase formation [Fig. 8(a)]; the film is poorly crystallized. Some other authors have also observed this behavior;[18,19] the crystallization quality of the PZT films seems directly related to the titanium oxydation degree. On a stabilized electrode, pure perovskite phase was obtained and the film is well crystallized [Fig. 8(b)]. It has become evident that the underlying metallization can significantly influence the crystallization of the PZT films.

3.3 Electrical measurements

Pt top electrodes with a diameter of 150 μm were deposited on the PZT films (lift-off process) to measure the electrical properties.

The PZT films deposited on encapsulated bottom electrodes cannot be characterized since all the contacts displayed a tendency for electrical shorts induced by the presence of platinum hillocks and so the electrical measurements are focused on films deposited on stabilized electrodes. We have determined the relative dielectric constant and the dissipation factor of PZT films as a function of film thickness. The relative dielectric constant and the dissipation factor of films between 0·15 and 3·3 μm thick is shown in Fig. 9 measured at 1 kHz by a multifrequency LCR meter. The relative dielectric constant (ε_r) increases with thickness, saturating at 750 for film thicknesses of 1·3 μm and above. A drop in dissipation factor is noted with increasing film thickness. A similar dependence has been observed by other authors who attributed this phenomenom to the presence of a transition layer between the film and the substrate.[20,21] In a more general sense, the presence of a very thin layer with a low ε_r will have a very large effect on the net ε_r.

The relative dielectric constant and the dissipation factor were also measured as functions of frequency (LCR meter, model HP4284A) and the results are summarized in Fig. 10(a) and (b), respectively. In this example, the PZT film thickness is 0·53 μm. We can observe a slight decrease in the dielectric constant at higher frequencies which is consistent with the expected normal frequency dependence.[22] The dielectric loss factor was nearly constant; tan δ varied between 2 and 5% in the frequency range 1 kHz–1 MHz.

Figure 11 represents the current density–voltage (J–V) characteristics of 0·15 μm [Fig. 11(a)] and 0·53 μm [Fig. 11(b)] thick PZT films. An initial leakage current density of less than 10^{-7} A cm^{-2} was measured on PZT film 0·53 μm thick and a flat and saturation region in this J–V curve appears in the range 4–10 V. Even under an applied voltage of 10 V, the leakage current density is limited to 10^{-7} A cm^{-2}. With decreasing thickness, the leakage current density was increased; at 2 V, J was higher than 10^{-6} A cm^{-2} for a 0·15 μm thick PZT film (instead of 10^{-8} A cm^{-2} for 0·53 μm thickness).

To examine the ferroelectric behavior of films and in particular their dependence with the film thicknesses, the polarization switching was observed using a RT6000 standart test system (from Radian technologies).

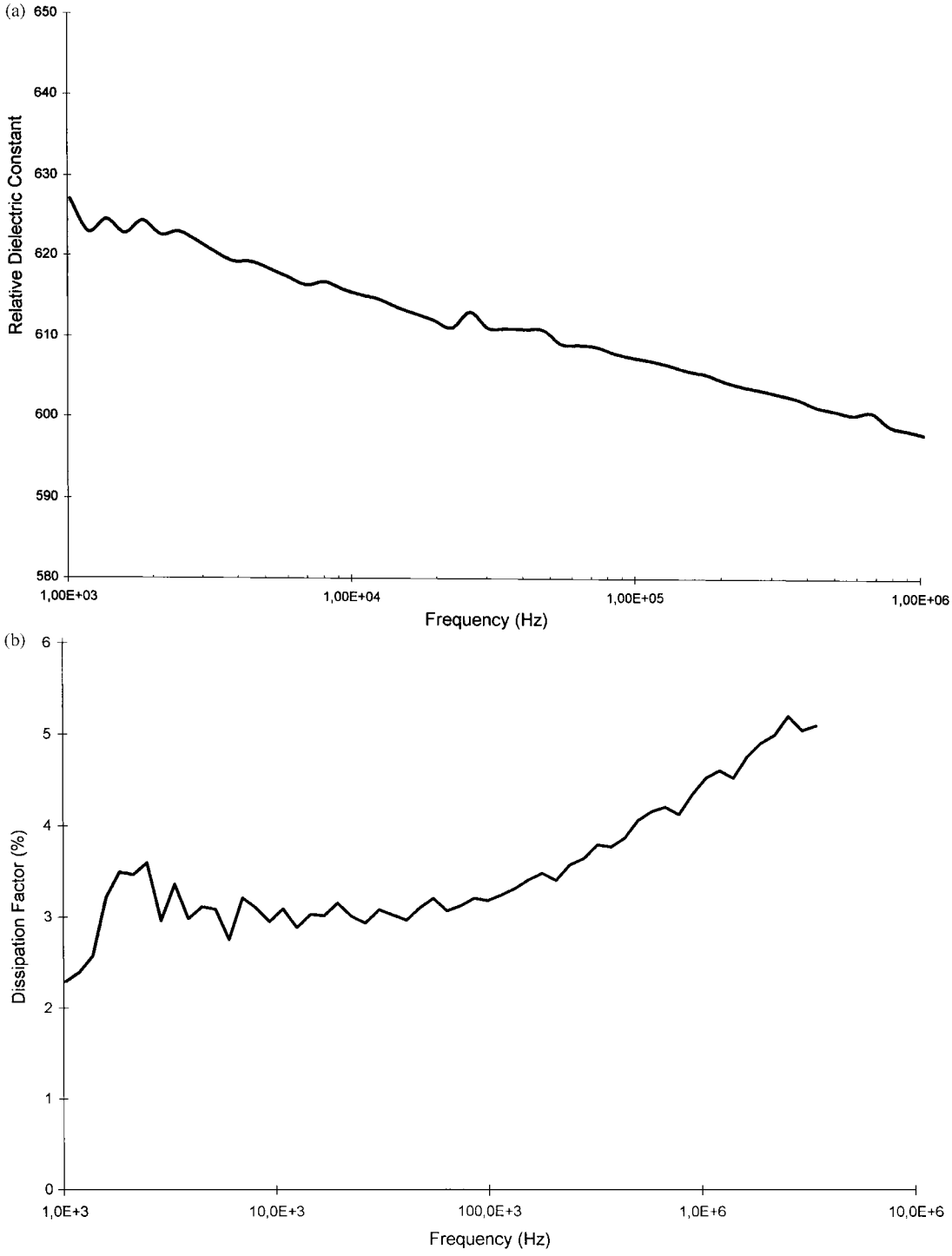

Fig. 10. Frequency dependence of: (a) dielectric constant and (b) dissipation factor of PZT film. Film was approximately 0·53 μm.

The averaged values of the coercive field E_c (more precisely E_c^+) and the remanent polarization P_r (more precisely P_r^+) are shown versus thickness in Fig. 12. The remanent polarization increased with the film thickness while the coercive fields decreased; if the film thickness is higher than 1·4 μm E_c and P_r are constant: 25 kV cm^{-1} and 19 μC cm^{-2}, respectively. These results confirm the expectation that the film properties improve with increasing thickness. The measured values in the films are higher for E_c and lower for P_r than those of ceramics with the same composition. These characteristics have been attributed to the effects of clamping of the film to the substrate and to the influence of the boundary between the film and the substrate (existence of a transition layer).

The hysteresis loops for all the films characterized in this study showed a shift along the axis of the electric field. Asymmetric hysteresis loops have been observed by many workers in both bulk ceramics and thin films and originate from internal field due to space-charge accumulation at the grain boundaries and at the film–electrode (top and bottom) interfaces.[23]

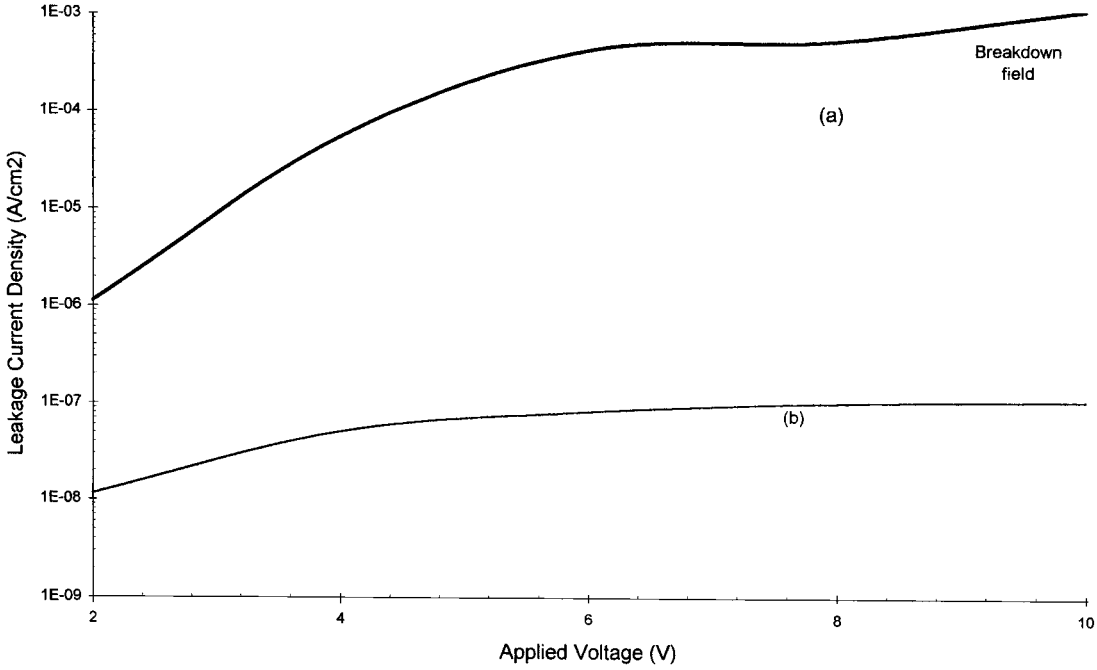

Fig. 11. Leakage current characteristics of PZT films: (a) 0·15 μm, (b) 0·53 μm thick.

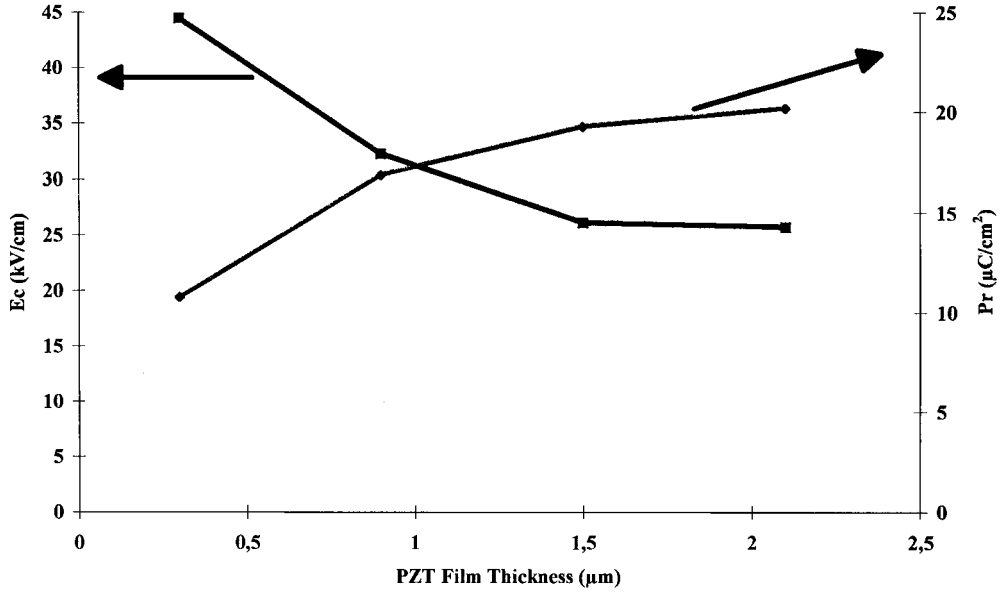

Fig. 12. Thickness dependence of hysteresis properties of PZT films.

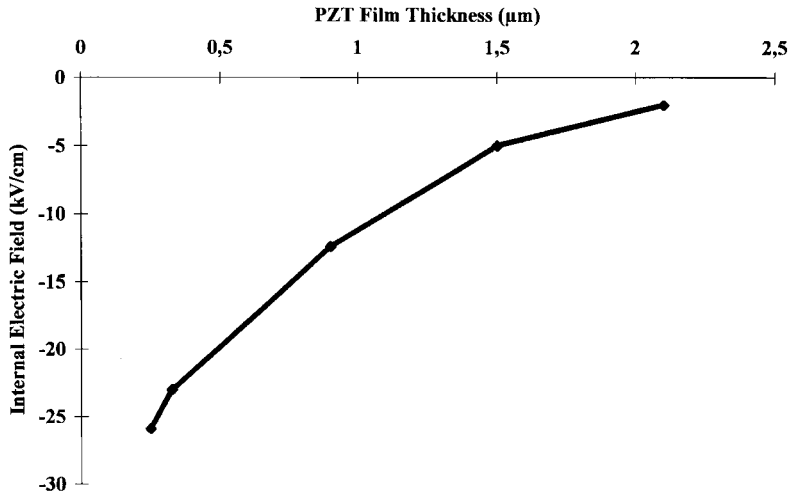

Fig. 13. Thickness dependence of the internal electric field magnitude.

We have observed that the magnitude of the internal field, i.e. the magnitude of the asymmetry, measured by $E_c^+ + E_c^-/2$, where E_c^+ and E_c^- are the positive and negative coercive field, respectively, is thickness dependent (Fig. 13). Its magnitude varied from about 25 to about 2 kV cm^{-1} when the thickness varied from 0·15 to 2·2 μm. The direction of the internal field was the same in all measured samples directing from the bottom to the top electrode. The disappearance of the internal field when the film thickness increased could be a consequence of the grain size variations with the film thickness[24,25] and the stresses stored in film which varied also with the film thickness. We have shown recently that this behavior can be related to the space charge located at the film–electrode interfaces.[26]

4 Conclusion

$Si/SiO_2/Ti/Pt$ substrates undergo chemical and microstructural changes during annealing at temperatures typically utilized for the preparation of PZT thin films. These include the migration of Ti through the Pt layer and the formation of defects (hillocks). The movement of Ti may be deleterious to the observed structural and electrical properties of the PZT thin films. The stabilization of the bottom electrode was achieved by replacing TiO_x layer instead of Ti layer. The study of the thickness dependence of the electrical properties of the PZT films has demonstrated that reduction in film thickness leads to the following: reduction in the relative dielectric constant and remanent polarization and increase in the loss tangent and coercive field. Nearly symmetric hysteresis loops, i.e. a reduction of the internal electric field, were observed when the film thickness increased.

Acknowledgements

The authors would like to thank P. Ossart from CNET Bagneux for Auger measurements and the Nord-Pas de Calais Country for his partial financial support.

References

1. Kingon, A. I., Streiffer, S. K., Basceri, C. and Summerfelt, S. R., *Mater. Res. Bull.*, 1996, **71**, 46.
2. Kojima, M., Sunagawa, M., Seto, H., Matsui, Y. and Hamakawa, Y., *Jpn. J. Appl. Phys.*, 1982, **22**, 255.
3. Okuyama, M. and Hamakawa, Y., *Ferroelectrics*, 1985, **63**, 243.
4. Araujo, C. A., Mc Millan, L. D., Melnick, B. M., Cuchiaro, J. D. and Scott, L. F., *Ferroelectrics*, 1990, **104**, 241.
5. Olowolafe, J. O., Jones, R. E. Jr, Campbell, A. C., Hedge, R. I. and Mogab, C. J., *J. Appl. Phys.*, 1993, **73**, 1764.
6. Fox, G. R., Trolier-McKinstry, S. and Krupanidhi, S. B., *J. Mater. Res.*, 1995, **10**, 1508.
7. Al-Shareef, H. N., Gifford, K. D., Rou, S. H., Hren, P. D., Auciello, O. and Kingon, A. I., *Int. Ferroelectrics*, 1993, **3**, 321.
8. Rèmiens, D., Jaber, B., Tirlet, J. F., Joire, H., Thierry, B. and Moriamez, Cl., *J. Eur. Ceram. Soc.*, 1994, **13**, 493.
9. Klee, M., Eusemann, R., Waser, R. and Setter, N., *J. Appl. Phys.*, 1992, **72**, 1566.
10. Torii, K., Kaga, T., Kushida, K., Takeuchi, H. and Takeda, E., *Jpn. J. Appl. Phys.*, 1991, **30**, 3562.
11. Sreenivas, K., Reaney, I., Maeder, T. and Setter, N., *J. Appl. Phys.*, 1994, **75**, 232.
12. Chung, S., Kim, J. W., Kim, G. H., Park, C. O. and Lee, W. J., *Jpn. J. Appl. Phys.*, 1997, **36**, 4386.
13. Kim, S. T., Kim, H. H., Lee, M. Y. and Lee, W. J., *Jpn. J. Appl. Phys.*, 1997, **36**, 294.
14. Spierings, G. A. C. M., Van Zon, J. B. A. and Larsen, P. K., *Int. Ferroelectrics*, 1993, **3**, 283.
15. Summerfelt, R. S., Kotechi, D., Kingon, A. and Al-Shareef, H. N., *Mat. Res. Soc. Symp.*, 1995, **361**, 257.
16. Grill, A., Beach, D., Smart, C. and Kane, W., *Mat. Res. Soc. Symp. Proc.*, 1993, **310**, 189.
17. Hren, P. D., Rou, S. H., Al-Shareef, H. N., Ameen, M. S., Auciello, O. and Kingon, A. I., *Int. Ferroelectrics*, 1992, **2**, 311.
18. Nam, Hyo-Ern, Kim, Hyun-Ho and Lee, Win-Jong., *Jpn. J. Appl. Phys.*, 1998, **37**, 3462.
19. Muralt, P., Maeder, T., Sagalowicz, L. and Hiboux, S., *J. Appl. Phys.*, 1998, **83**, 3835.
20. Roy, R. A. and Etzold, K. F., *J. Mater. Res.*, 1992, **7**, 1455.
21. Dana, S. S., Etzold, K. F. and Glabes, J. G., *J. Appl. Phys.*, 1991, **69**, 4398.
22. Jonscher, A. K., In *Physics of Thin Films*, Vol. II, ed. G. Hass and M. H. Francombe. Academic Press, New York, 1980, 205.
23. Fukami, T. and Fujii, F., *Jpn. J. Appl. Phys.*, 1985, **24**, 632.
24. Rèmiens, D., Jaber, B., Tronc, P. and Thierry, B., *J. Eur. Ceram. Soc.*, 1996, **16**, 467.
25. Beach, D. B., Laibowitz, R. B., Shaw, T. M., Grill, A. and Kane, W. K., *Int. Ferroelectrics*, 1995, **7**, 161.
26. Baudry, L., Cattan, E., Vélu, G., Tournier, J., Rémiens, D., Proc. of the IV European Conf. on Applications of Polar Dielectrics in Ferroelectrics, Montreux, 24–27 August 1998, 485.